

Bias as a Virtue: Rethinking Generalization under Distribution Shifts

Ruixuan Chen *
Tsinghua University

Wentao Li
Tsinghua University

Jiahui Xiao
Tsinghua University

Yuchen Li
Tsinghua University

Yimin Tang
University of Southern California

Xiaonan Wang *[†]
Tsinghua University

Abstract

Machine learning models often degrade when deployed on data distributions different from their training data. Challenging conventional validation paradigms, we demonstrate that higher in-distribution (ID) bias can lead to better out-of-distribution (OOD) generalization. Our Adaptive Distribution Bridge (ADB) framework implements this insight by introducing controlled statistical diversity during training, enabling models to develop bias profiles that effectively generalize across distributions. Empirically, we observe a robust negative correlation where higher ID bias corresponds to lower OOD error—a finding that contradicts standard practices focused on minimizing validation error. Evaluation on multiple datasets shows our approach significantly improves OOD generalization. ADB achieves robust mean error reductions of up to 26.8% compared to traditional cross-validation, and consistently identifies high-performing training strategies, evidenced by percentile ranks often exceeding 74.4%. Our work provides both a practical method for improving generalization and a theoretical framework for reconsidering the role of bias in robust machine learning.

1 Introduction

Machine learning models frequently suffer performance degradation when deployed in environments with distributions different from their training data [24, 34]. This distribution shift problem is particularly acute in scientific discovery domains where training data encompasses only limited experimental spaces, or real-world applications like finance where historical data often differs systematically from future market conditions [19].

Traditional approaches to model selection rely on cross-validation, which implicitly assumes that models with lower in-distribution (ID) error will generalize better to out-of-distribution (OOD) settings. However, mounting evidence suggests this assumption fails under significant distribution shifts [28, 12], creating a critical gap between theoretical expectations and practical performance.

We challenge this foundational practice by demonstrating that models with strategically increased ID bias can achieve significantly better OOD generalization. Our theoretical analysis reveals that when the bias diversity is appropriately calibrated relative to the distribution shift magnitude, the correlation between ID and OOD errors becomes negative. In this counterintuitive regime, conventional model selection criteria that minimize ID error paradoxically select models with worse OOD performance.

Building on this insight, we introduce the Adaptive Distribution Bridge (ADB) framework, which leverages controlled statistical diversity during training to enhance OOD generalization. ADB quanti-

*Contact: chenruixuan@mail.tsinghua.edu.cn, wangxiaonan@tsinghua.edu.cn

[†]Corresponding author

fies and selects training sequences using debiased optimal-transport distances, inducing appropriate bias variation without requiring explicit knowledge of target distributions. Our approach creates models whose inherent bias profiles effectively navigate distribution shifts while maintaining focus on invariant patterns.

Experiments across multiple domains show ADB achieves substantial mean OOD error reductions, for instance, by up to 26.8% in MAE on the T1S1 dataset using the Cumulative method (Table 1), when compared to traditional cross-validation. Our approach consistently identifies high-performing training strategies (with percentile ranks often above 74.4%). These findings validate our theoretical framework and offer a practical alternative to established validation paradigms.

Contributions: (1) We establish theoretical conditions under which higher ID bias leads to reduced OOD error; (2) We introduce the ADB framework implementing controlled statistical diversity during training; (3) We demonstrate empirically that our approach significantly outperforms standard cross-validation on multiple prediction tasks; (4) We establish a paradigm that reconceptualizes bias as a potential virtue for addressing distribution shifts.

2 Related Work

2.1 Bias-Variance Tradeoff and Model Selection

The bias-variance tradeoff represents a fundamental concept in statistical learning theory [7, 15]. Conventional model selection minimizes validation error as a proxy for generalization performance, underpinning cross-validation [2] across machine learning applications.

Recent work questions this orthodoxy in specific contexts. D’Amour et al. [6] highlighted how models with equivalent validation performance can behave drastically differently under distribution shifts. Kumar et al. [20] demonstrate that minimizing in-distribution error during fine-tuning can actively harm OOD performance, providing direct evidence for our thesis. Efforts to improve robustness include seeking invariant features across environments [1], employing ensemble methods for bias diversity [35], and leveraging feature-level diversity [14], all of which contribute to reconsidering bias as a potential virtue rather than a pure detriment.

Our work builds upon these insights by proposing a novel framework that, instead of solely focusing on bias minimization or feature invariance, strategically manages and leverages controlled bias variation to enhance generalization under distribution shifts.

2.2 Addressing Distribution Shifts

Existing approaches to distribution shifts include: domain adaptation methods [9, 36] that align feature distributions between source and target domains; robust optimization approaches [27, 8] that optimize for worst-case performance; and causality-based techniques [26, 30] that identify invariant causal mechanisms.

A key limitation across these approaches is their dependence on specific knowledge about target distributions or precise characterization of shift types. Recent benchmarks and evaluations [37, 29, 33] demonstrate that many existing methods fail to generalize reliably across diverse real-world distribution shifts. ADB addresses these limitations by introducing controlled diversity during training without requiring explicit knowledge of target distributions.

2.3 Training Dynamics and Sequence Manipulation

How models interact with training data—particularly the order and composition of training batches—significantly impacts learning outcomes. Curriculum learning [3, 11] arranges examples by difficulty, while active learning [32, 31] iteratively selects informative examples. Recent work by Mindermann et al. [23] demonstrates the benefits of prioritizing training on points that are learnable, worth learning, and not yet learned, showing how strategic data selection affects generalization. Killamsetty et al. [16] propose gradient-matching approaches for efficient training data subset selection, further establishing the importance of data presentation strategies.

ADB differs from these approaches by focusing on distributional characteristics of entire training sequences rather than example-level properties. Unlike methods that typically assess individual

examples or local batch compositions, ADB uniquely quantifies the evolving distributional characteristics of training subsequences derived from permutations in relation to the overall distribution of the training dataset. While previous work has observed how training order affects generalization [13], ADB provides a theoretical foundation linking sequence diversity to bias profiles and explicitly quantifies these relationships using optimal transport distances. This enables systematic induction of controlled bias variation beneficial for OOD generalization, aligning with recent data-centric AI perspectives [38] that emphasize the central role of data management in model performance.

3 Theoretical Foundation: Bias Under Distribution Shifts

3.1 Mean Shift Model

We analyze a simplified model where error metrics in training and test distributions are generated as:

$$\mathcal{E}_{\text{train}} = \mu_{\text{train}} + \epsilon, \quad \epsilon \sim \mathcal{N}(0, \sigma_{\text{train}}^2), \quad (1)$$

$$\mathcal{E}_{\text{test}} = \mu_{\text{test}} + \epsilon', \quad \epsilon' \sim \mathcal{N}(0, \sigma_{\text{test}}^2), \quad (2)$$

with a positive mean shift $\Delta = \mu_{\text{test}} - \mu_{\text{train}} > 0$, representing the common scenario where models perform worse on test data than training data due to distribution shifts.

We consider candidate models whose expected error deviates from the training mean μ_{train} by a bias parameter b . Traditional cross-validation prioritizes models with b near zero to minimize ID error. However, when $b = 0$, with mean square error metric, the OOD error becomes Δ^2 , which can be substantial when the shift Δ is significant.

3.2 Correlation Between ID and OOD Errors

For a model with bias parameter b , we define $T(b) = b^2$ (ID error component) and $U(b) = (b - \Delta)^2$ (OOD error component).

We model b as following a half-normal distribution with scale parameter k . Let $\alpha = \sqrt{\frac{2}{\pi}}$. The half-normal probability density function is:

$$f(b; k) = \begin{cases} \frac{\alpha}{k} \exp\left(-\frac{b^2}{2k^2}\right), & \text{if } b \geq 0 \\ 0, & \text{if } b < 0 \end{cases} \quad (3)$$

where k represents bias variation across model populations.

We select the half-normal distribution for three key reasons: (1) it restricts the bias parameter to non-negative values, reflecting the practical scenario where we eliminate underfitting models during training; (2) it provides a single parameter k that directly controls the spread of bias variation, enabling clear analysis of the relationship between bias diversity and OOD performance; and (3) it has well-understood statistical properties that allow for closed-form derivation of the correlation between ID and OOD errors.

Through mathematical derivation (Appendix A), we prove that the Pearson correlation coefficient $\rho_{T,U}$ between $T(b)$ and $U(b)$ becomes negative when $k < \alpha\Delta$.

This condition explains both standard (non-shifting) and distribution shift scenarios. In conventional i.i.d. settings ($\Delta \approx 0$), the inequality $k < \alpha\Delta$ is virtually impossible to satisfy since $k > 0$ by definition, explaining the typical positive correlation between ID and OOD errors. However, under significant distribution shifts where Δ is large, the condition $k < \alpha\Delta$ becomes feasible to satisfy, enabling negative correlation.

3.3 Optimizing the Bias-Diversity Tradeoff

When $k < \alpha\Delta$, the correlation $\rho_{T,U}$ is negative. As k increases within this range, $\rho_{T,U}$ increases toward zero, meaning the negative correlation weakens. Therefore, the most negative correlation occurs at the smallest feasible values of k .

This creates a practical tradeoff: we need k large enough to provide sufficient bias diversity for distribution shift compensation, yet small enough to maintain a strong negative correlation between ID and OOD errors.

The critical challenge is achieving this appropriate level of bias variation k in practice, which motivates our ADB framework.

4 Adaptive Distribution Bridge (ADB) Framework

4.1 Framework Motivation and Overview

Building on our theoretical finding that appropriate bias variation $k < \alpha\Delta$ improves OOD performance through negative ID-OOD error correlation, the ADB framework controls training sequences to indirectly influence k . We achieve this by quantifying the distributional characteristics of potential training sequences, categorizing these sequences based on their statistical diversity, and identifying sequences that induce appropriate bias variation for effective OOD generalization. The core intuition is that by exposing the model to training sequences with varying degrees of statistical divergence from the global data distribution, we can prevent premature convergence to a narrow set of features and thereby modulate the model’s learned bias profile, akin to influencing the bias variation parameter k from our theoretical model.

4.2 Problem Formulation

Let $\mathcal{D} = \{(x_i, y_i)\}_{i=1}^N$ be a dataset of N samples. We train a model $f_\theta : \mathcal{X} \rightarrow \mathcal{Y}$ using mini-batch stochastic gradient descent. A permutation π defines a training sequence, with batches defined as:

$$B_t^\pi = \left\{ (x_{\pi((t-1)B+j)}, y_{\pi((t-1)B+j)}) : j = 1, 2, \dots, \min(B, N - (t-1)B) \right\} \quad (4)$$

where B is the batch size and t indexes the training step.

Our objective is to identify permutations that introduce the appropriate level of statistical diversity to induce beneficial bias variation k that enhances model robustness under distribution shifts.

4.3 Distributional Diversity Quantification

To quantify distributional diversity, we represent data samples in a space where distributional distances are meaningful, measure the deviation between training batches (or cumulative subsets) and the global training distribution, and categorize permutations based on their deviation patterns.

For high-dimensional problems, we employ a Variational Autoencoder (VAE) [18] to map features to a lower-dimensional latent space for efficient distance computation.

We quantify statistical divergence using the Sinkhorn distance [5], which provides a computationally tractable approximation to the Wasserstein-1 distance (W_1):

$$W_\epsilon(\mu_S, \mu_G) = \langle \mathbf{C}, \mathbf{P}^* \rangle \quad (5)$$

where \mathbf{C} is the cost matrix with elements $C_{ij} = \|z_i - z_j\|_1$ and the optimal transport plan \mathbf{P}^* is:

$$\mathbf{P}^* = \arg \min_{\mathbf{P} \in \Pi(\mu_S, \mu_G)} \left\{ \langle \mathbf{C}, \mathbf{P} \rangle - \epsilon H(\mathbf{P}) \right\} \quad (6)$$

Here, μ_S and μ_G represent the empirical probability distributions of a sample subset and the global training set, respectively. $\Pi(\mu_S, \mu_G)$ is the set of all transport plans between these distributions, and $H(\mathbf{P}) = -\sum_{i,j} P_{ij} \log P_{ij}$ is the entropy of the transport plan.

To mitigate entropic bias, we compute the debiased distance:

$$W_{\text{debiased}}(\mu_S, \mu_G) = 2W_\epsilon(\mu_S, \mu_G) - W_\epsilon(\mu_S, \mu_S) - W_\epsilon(\mu_G, \mu_G) \quad (7)$$

4.4 Computational Approaches

We introduce two approaches for computing distributional deviations (Algorithm 1):

Cumulative Evaluation This approach evaluates the distance between the cumulative subset of samples seen up to step t and the global training distribution:

$$D_t^\pi = W_{\text{debiased}}(\mu_{S_t^\pi}, \mu_G), \text{ where } S_t^\pi = \{\pi(1), \pi(2), \dots, \pi(tB)\} \quad (8)$$

Batchwise Computation This approach computes the deviation of individual batches from the global training distribution:

$$D_t^\pi = W_{\text{debiased}}(\mu_{B_t^\pi}, \mu_G) \quad (9)$$

4.5 Permutation Classification

For each time step t , we compute the mean $\mu_{D,t}$ and standard deviation $\sigma_{D,t}$ of the distributional deviations across all permutations. We then count the number of times each permutation’s deviation falls outside the $\pm 2\sigma$ bounds:

$$O^{\pi_m} = \sum_{t=1}^T \mathbf{1}(D_t^{\pi_m} \notin [\mu_{D,t} - 2\sigma_{D,t}, \mu_{D,t} + 2\sigma_{D,t}]) \quad (10)$$

Based on these counts, we classify permutations into three categories:

- Low deviation ($O^\pi \leq \tau_{\text{low}}$): Maintains tight alignment with the global training distribution
- Medium deviation ($\tau_{\text{low}} < O^\pi \leq \tau_{\text{high}}$): Provides moderate statistical diversity
- High deviation ($O^\pi > \tau_{\text{high}}$): Exhibits substantial distributional deviations

We determine thresholds τ_{low} and τ_{high} using distribution quantiles of the empirical distribution of outlier counts (O^π). We observed distinct patterns for the two computational approaches across datasets. For the Cumulative method, this empirical distribution consistently exhibits a pattern resembling exponential decay for low outlier counts, while the high end consists primarily of outlier values. For the Batchwise method, the empirical distribution approximates a normal distribution. The probability distribution across deviation groups and specific threshold values for both approaches are detailed in Appendix B, Table 3.

Algorithm 1 ADB Framework

Require: Dataset latent representations $\{z_i\}_{i=1}^N$, batch size B , permutations count M , mode \in {cumulative, batchwise}
Ensure: Permutation sets $\Pi_{\text{low}}, \Pi_{\text{med}}, \Pi_{\text{high}}$

- 1: Generate M random permutations $\{\pi_1, \pi_2, \dots, \pi_M\}$
- 2: $T \leftarrow \lceil N/B \rceil$
- 3: **for** $m = 1$ **to** M **do**
- 4: **for** $t = 1$ **to** T **do**
- 5: **if** mode = cumulative **then**
- 6: $S_t^{\pi_m} \leftarrow \{z_{\pi_m(1)}, \dots, z_{\pi_m(tB)}\}$
- 7: $D_t^{\pi_m} \leftarrow W_{\text{debiased}}(\mu_{S_t^{\pi_m}}, \mu_G)$
- 8: **else**
- 9: $B_t^{\pi_m} \leftarrow \{z_{\pi_m((t-1)B+1)}, \dots, z_{\pi_m(\min(tB, N))}\}$
- 10: $D_t^{\pi_m} \leftarrow W_{\text{debiased}}(\mu_{B_t^{\pi_m}}, \mu_G)$
- 11: **end if**
- 12: **end for**
- 13: **end for**
- 14: **for** $t = 1$ **to** T **do**
- 15: $\mu_{D,t} \leftarrow \frac{1}{M} \sum_{m=1}^M D_t^{\pi_m}$
- 16: $\sigma_{D,t} \leftarrow \sqrt{\frac{1}{M} \sum_{m=1}^M (D_t^{\pi_m} - \mu_{D,t})^2}$
- 17: **end for**
- 18: **for** $m = 1$ **to** M **do**
- 19: $O^{\pi_m} \leftarrow \sum_{t=1}^T \mathbf{1}(D_t^{\pi_m} \notin [\mu_{D,t} - 2\sigma_{D,t}, \mu_{D,t} + 2\sigma_{D,t}])$
- 20: **end for**
- 21: Determine thresholds τ_{low} and τ_{high} using distribution quantiles
- 22: $\Pi_{\text{low}} \leftarrow \{\pi_m : O^{\pi_m} \leq \tau_{\text{low}}\}$
- 23: $\Pi_{\text{med}} \leftarrow \{\pi_m : \tau_{\text{low}} < O^{\pi_m} \leq \tau_{\text{high}}\}$
- 24: $\Pi_{\text{high}} \leftarrow \{\pi_m : O^{\pi_m} > \tau_{\text{high}}\}$
- 25: **return** $\Pi_{\text{low}}, \Pi_{\text{med}}, \Pi_{\text{high}}$

5 Experimental Results

5.1 Experimental Setup

We evaluate our approach on three datasets: T1S1 (molecular property prediction; currently a private dataset, planned for public release) and Year Prediction MSD [4] (audio features from 515k songs).

To evaluate generalization under distribution shifts, OOD test sets are created using stratified sampling. Training and test sets are normalized separately, resulting in W_1 distances in label space between OOD distributions ranging from 0.61 to 0.86, ensuring meaningful distribution shifts (detailed W_1 measurements in Appendix B). For instance, the T1S1 dataset (564,220 molecules) has its OOD test set (64,220 molecules) formed via this stratified sampling. The remaining 500,000 molecules are divided into a 490,000-sample training set and a 10,000-sample in-distribution (ID) validation set; the validation set is kept small to minimize disruption to training distribution properties. For MSD dataset, we use 90,000 samples for training, 10,000 samples for ID validation, and 10,000 samples for OOD testing, with all sets formed through the same stratified sampling approach.

Our ADB implementation processes the training samples as detailed in Algorithm 1 (with $M = 500$ permutations) to generate and classify these permutations into three deviation categories (Low, Medium, High) based on their statistical properties. Each category is evaluated by training 30 models per deviation group across each dataset. During training, each model uses 50 permutation sequences sampled from its assigned deviation category, with each sequence determining the training sample order for one epoch. This approach ensures consistent exposure to the designated level of statistical diversity throughout training.

The classification thresholds τ_{low} and τ_{high} , and the probability distribution across deviation groups, are detailed in Appendix B, Table 3.

The experimental protocol is as follows:

- **Optimization:** Models are trained using Adam [17] with learning rate 0.001 for 50 epochs.
- **Batch sizes:** We use batch size B of 5000 for T1S1 and 1000 for MSD (corresponding to the batch size parameter in ADB), each representing approximately 1% of their respective training set sizes.
- **Architecture:** For molecular datasets (T1S1), we use message-passing neural networks following [10], while MSD uses fully-connected networks.
- **Dimensionality reduction for ADB:** To facilitate distance computations in the ADB framework, Variational Autoencoders (VAEs) are employed. For molecular datasets (T1S1), VAEs map 2098 input features (constructed from Morgan fingerprints [25] and RDKit molecular properties [21]) to a 32-dimensional latent space using a six-hidden-layer encoder architecture with power-of-2 dimension reduction. For the MSD dataset, VAEs map 90 input features to an 8-dimensional latent space via a three-hidden-layer encoder.
- **Optimal transport:** Sinkhorn algorithm with entropic regularization parameter $\epsilon = 0.05$.

Performance is assessed using Mean Absolute Error (MAE) and Root Mean Square Error (RMSE), with 10-fold cross-validation as the benchmark.

5.2 Performance Comparison

Table 1 presents the effectiveness of our ADB framework compared to standard 10-fold cross-validation (CV). The percentage improvement (I) quantifies ADB’s relative advantage over CV, while the percentile rank (PR) positions the ADB model within the distribution of all possible training permutations, with higher percentages indicating better relative performance. All performance improvements are statistically significant ($p < 0.05$) as demonstrated through paired t-tests (see Appendix B.4).

The results demonstrate a clear advantage for ADB over traditional CV. The Batchwise approach shows significant improvements in both MAE and RMSE, while the Cumulative approach delivers even stronger improvements with metrics ranking above the 74th percentile. The Cumulative approach consistently outperforms Batchwise because it accounts for the full historical sequence of training samples rather than isolated batches.

Notably, MAE improvements consistently exceed RMSE gains across both methods, demonstrating MAE’s superior statistical robustness under distribution shifts due to its reduced sensitivity to outliers.

It is also worth noting that while the absolute percentage improvement (I) varies across datasets due to their distinct characteristics, the percentile rank (PR) remains consistently high, particularly for the Cumulative approach. This suggests that ADB reliably identifies high-performing permutation strategies relative to the entire space of possibilities, regardless of the specific dataset.

Our ADB framework favors Medium and High deviation groups, as these typically provide greater statistical diversity beneficial for robust OOD generalization. For Table 1, we sample 10 models proportionally from the Medium and High groups, select the one with the highest ID error, and report its OOD performance. Performance data for all deviation groups is available in Appendix B.3.

Table 1: Performance evaluation of the ADB approach

Method	Dataset	Metric	CV↓	ADB↓	I (%)↑	PR (%)↑
Batchwise	T1S1	MAE	0.478 ± 0.018	0.427 ± 0.007	10.7	83.4
		RMSE	0.561 ± 0.013	0.521 ± 0.007	7.2	76.9
	MSD	MAE	0.868 ± 0.005	0.854 ± 0.001	1.55	85.2
		RMSE	1.163 ± 0.007	1.149 ± 0.002	1.22	70.5
Cumulative	T1S1	MAE	0.514 ± 0.020	0.365 ± 0.003	26.8	91.2
		RMSE	0.554 ± 0.017	0.459 ± 0.003	17.2	85.7
	MSD	MAE	0.874 ± 0.001	0.850 ± 0.001	2.96	91.2
		RMSE	1.159 ± 0.005	1.138 ± 0.001	1.81	91.1

5.3 Distribution-Error Relationship Analysis

Our analysis demonstrates that under negative correlation between ID and OOD errors (when $k < \alpha\Delta$), standard cross-validation that minimizes ID error leads to suboptimal OOD performance. In such cases, models with higher ID error can achieve lower OOD error.

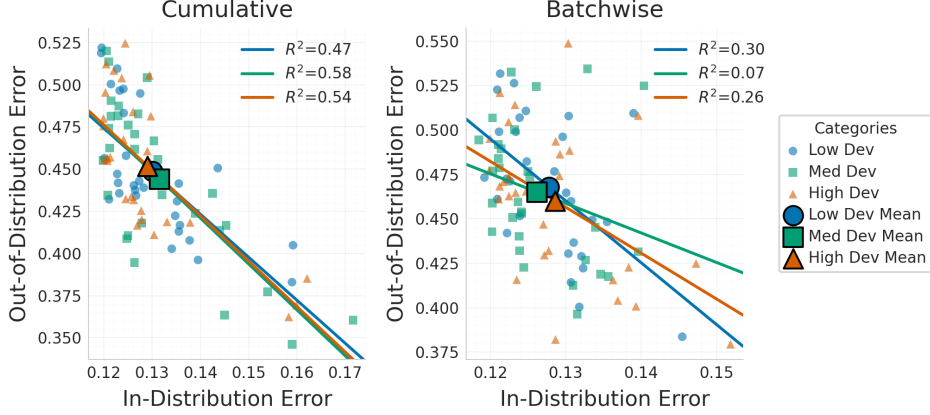


Figure 1: Relationship between in-distribution and out-of-distribution MAE across Low, Medium, and High deviation groups for T1S1 with both computational approaches. The negative correlation is evident, with distinct patterns for each group that reveal the underlying bias-diversity tradeoff.

Based on the negative ID-OOD correlation patterns observed in Figure 1, we focus on Medium and High deviation groups for model selection. By selecting the highest ID error model from these groups, ADB leverages this correlation pattern to improve OOD performance.

This empirical finding aligns with our theoretical model (Section 3), which predicts that when $k < \alpha\Delta$, increased bias diversity can lead to improved OOD outcomes through negative ID-OOD correlation. The High deviation group exhibits larger k (more bias diversity) but potentially weaker correlation strength, while the Medium group provides moderate k with potentially stronger negative correlation. ADB’s selection of the maximum ID error model effectively navigates this tradeoff without requiring precise knowledge of the optimal bias diversity level.

5.4 Computational Efficiency

The batchwise approach achieves substantial computational speedup compared to the cumulative approach, but at a significant performance cost as evident in our experimental results.

For computational complexity, let N be sample count and B be batch size. With the Sinkhorn algorithm for optimal transport having complexity $O(nm \log(nm)/\epsilon^2)$ for distributions with n and m points [22], where ϵ controls the entropic regularization:

$$C_{\text{cumulative}} = \sum_{t=1}^{N/B} O((tB)N \log(tBN)/\epsilon^2) = O\left(\frac{N^3 \log N}{B\epsilon^2}\right) \quad (11)$$

$$C_{\text{batchwise}} = \sum_{t=1}^{N/B} O(BN \log(BN)/\epsilon^2) = O\left(\frac{N^2 \log N}{\epsilon^2}\right) \quad (12)$$

With $B = 0.01N$, this yields a theoretical upper bound on speedup of approximately 100 \times . In practice, our empirical observations show speedups between 1.9 \times and 4.1 \times due to implementation considerations. For computational efficiency, our permutation analysis leverages parallel computation, with Monte Carlo simulations achieving linear speedup across multiple GPU resources.

Table 2: ADB computational efficiency comparison on H800 GPUs (GPU hours per permutation)

Dataset Size	Method	Computation Time	Relative Speedup
100,000 \times 8	Cumulative	0.131	1.0 \times
	Batchwise	0.070	1.9 \times
100,000 \times 32	Cumulative	0.151	1.0 \times
	Batchwise	0.037	4.1 \times
500,000 \times 32	Cumulative	1.480	1.0 \times
	Batchwise	0.533	2.8 \times

For our largest dataset (500,000 samples), processing all 500 permutation paths required 266.5 total GPU hours with the batchwise approach versus 740 hours with the cumulative approach across 5 H800 GPUs.

6 Discussion and Conclusion

Our work demonstrates that higher ID bias can improve OOD generalization, challenging conventional validation paradigms. The ADB framework provides a practical implementation of this principle through controlled statistical diversity during training.

Key implications include:

- **Validation paradigm shift:** Traditional approaches that minimize ID error may harm generalization under distribution shifts. Our results demonstrate that cross-validation can lead to substantially higher OOD error, while our ADB framework yields significant mean improvements and consistently identifies high-performing strategies.
- **Practical framework:** ADB enhances model robustness while requiring only an awareness of distribution shifts within a reasonable range, without requiring detailed knowledge of their specific characteristics.
- **Theoretical foundation:** Our analysis linking ID bias and OOD error provides a basis for rethinking bias in machine learning.

Limitations and future work include further theoretical development, investigating how dataset characteristics and computational approaches influence the quantitative relationship between induced distributional deviation levels and the resulting bias-diversity tradeoff. The distributional diversity principles introduced in this work could potentially inform other machine learning paradigms where training dynamics and data selection play crucial roles, particularly in active learning, curriculum learning, and robust transfer learning scenarios. Code for the ADB framework and experiments will be made publicly available upon publication.

References

- [1] Martin Arjovsky, Léon Bottou, Ishaan Gulrajani, and David Lopez-Paz. Invariant risk minimization. *arXiv preprint arXiv:1907.02893*, 2019.

- [2] Sylvain Arlot and Alain Celisse. A survey of cross-validation procedures for model selection. *Statistics surveys*, 4:40–79, 2010.
- [3] Yoshua Bengio, Jérôme Louradour, Ronan Collobert, and Jason Weston. Curriculum learning. In *Proceedings of the 26th Annual International Conference on Machine Learning*, pages 41–48, 2009.
- [4] Thierry Bertin-Mahieux, Daniel P.W. Ellis, Brian Whitman, and Paul Lamere. The million song dataset. In *Proceedings of the 12th International Society for Music Information Retrieval Conference (ISMIR)*, pages 591–596, Miami, Florida, 2011.
- [5] Marco Cuturi. Sinkhorn distances: Lightspeed computation of optimal transport. In *Advances in Neural Information Processing Systems*, volume 26, 2013.
- [6] Alexander D’Amour, Katherine Heller, Dan Moldovan, Ben Adlam, Babak Alipanahi, Alex Beutel, Christina Chen, Jonathan Deaton, Jacob Eisenstein, Matthew D Hoffman, et al. Under-specification presents challenges for credibility in modern machine learning. *arXiv preprint arXiv:2011.03395*, 2020.
- [7] Pedro Domingos. A unified bias-variance decomposition. *Proceedings of 17th International Conference on Machine Learning*, pages 231–238, 2000.
- [8] John C Duchi and Hongseok Namkoong. Learning models with uniform performance via distributionally robust optimization. In *Advances in Neural Information Processing Systems*, volume 31, 2018.
- [9] Yaroslav Ganin, Evgeniya Ustinova, Hana Ajakan, Pascal Germain, Hugo Larochelle, François Laviolette, Mario Marchand, and Victor Lempitsky. Domain-adversarial training of neural networks. *The Journal of Machine Learning Research*, 17(1):2096–2030, 2016.
- [10] Justin Gilmer, Samuel S Schoenholz, Patrick F Riley, Oriol Vinyals, and George E Dahl. Neural message passing for quantum chemistry. In *International Conference on Machine Learning*, pages 1263–1272. PMLR, 2017.
- [11] Alex Graves, Marc G Bellemare, Jacob Menick, Remi Munos, and Koray Kavukcuoglu. Automated curriculum learning for neural networks. In *International Conference on Machine Learning*, pages 1311–1320. PMLR, 2017.
- [12] Ishaan Gulrajani and David Lopez-Paz. In search of lost domain generalization. In *International Conference on Learning Representations*, 2021.
- [13] Guy Hacohen and Daphna Weinshall. On the power of curriculum learning in training deep networks. In *International Conference on Machine Learning*, pages 2535–2544. PMLR, 2019.
- [14] Pavel Izmailov, Dmitry Podoprikin, Timur Garipov, Dmitry Vetrov, and Andrew Gordon Wilson. Feature-level ensembling for both accuracy and robustness. In *International Conference on Machine Learning*, pages 9981–9991. PMLR, 2022.
- [15] Gareth M James. Variance and bias for general loss functions. *Machine learning*, 51(2):115–135, 2003.
- [16] Krishnateja Killamsetty, Durga Sivasubramanian, Ganesh Ramakrishnan, and Rishabh Iyer. Grad-match: Gradient matching based data subset selection for efficient deep model training. In *International Conference on Machine Learning*, pages 5464–5474. PMLR, 2021.
- [17] Diederik P Kingma and Jimmy Ba. Adam: A method for stochastic optimization. In *International Conference on Learning Representations*, 2014.
- [18] Diederik P Kingma and Max Welling. Auto-encoding variational bayes. In *International Conference on Learning Representations*, 2013.
- [19] Pang Wei Koh, Shiori Sagawa, Henrik Marklund, Sang Michael Xie, Marvin Zhang, Akshay Balsubramani, Weihua Xu, Percy Liang, et al. Wilds: A benchmark of in-the-wild distribution shifts. *International Conference on Machine Learning*, pages 5637–5664, 2021.

- [20] Ananya Kumar, Aditi Raghunathan, Roy Jones, Tengyu Ma, and Percy Liang. Fine-tuning can distort pretrained features and underperform out-of-distribution. In *International Conference on Learning Representations*, 2022.
- [21] Greg Landrum et al. Rdkit: Open-source cheminformatics. <http://www.rdkit.org>, 2013. Accessed: 2023-12-01.
- [22] Jianzhou Luo, Dingchuan Yang, and Ke Wei. Improved complexity analysis of the sinkhorn and greenkhorn algorithms for optimal transport. *arXiv preprint arXiv:2305.14939*, 2023.
- [23] Sören Mindermann, Jan Markus Brauner, Muhammad Tarek Razzak, Mrinank Sharma, Andreas Kirsch, Winnie Xu, Benedikt Hölten, Aidan N Gomez, Adrien Morisot, Sebastian Farquhar, and Yarin Gal. Prioritized training on points that are learnable, worth learning, and not yet learnt. In *International Conference on Machine Learning*, pages 15630–15649. PMLR, 2022.
- [24] Jose G Moreno-Torres, Troy Raeder, Rocío Alaiz-Rodríguez, Nitesh V Chawla, and Francisco Herrera. A unifying view on dataset shift in classification. *Pattern recognition*, 45(1):521–530, 2012.
- [25] Harry L Morgan. The generation of a unique machine description for chemical structures—a technique developed at chemical abstracts service. *Journal of Chemical Documentation*, 5(2):107–113, 1965.
- [26] Jonas Peters, Peter Bühlmann, and Nicolai Meinshausen. Causal inference using invariant prediction: identification and confidence intervals. *Journal of the Royal Statistical Society: Series B (Statistical Methodology)*, 78(5):947–1012, 2016.
- [27] Shiori Sagawa, Pang Wei Koh, Tatsunori B Hashimoto, and Percy Liang. Distributionally robust neural networks for group shifts: On the importance of regularization for worst-case generalization. In *International Conference on Learning Representations*, 2019.
- [28] Shiori Sagawa, Pang Wei Koh, Tatsunori B Hashimoto, and Percy Liang. An investigation of why overparameterization exacerbates spurious correlations. In *International Conference on Machine Learning*, pages 8346–8356. PMLR, 2020.
- [29] Shibani Santurkar, Dimitris Tsipras, and Aleksander Madry. Breeds: Benchmarks for sub-population shift. In *Advances in Neural Information Processing Systems*, volume 34, pages 10816–10830, 2021.
- [30] Bernhard Schölkopf, Francesco Locatello, Stefan Bauer, Nan Rosemary Ke, Nal Kalchbrenner, Anirudh Goyal, and Yoshua Bengio. Toward causal representation learning. *Proceedings of the IEEE*, 109(5):612–634, 2021.
- [31] Ozan Sener and Silvio Savarese. Active learning for convolutional neural networks: A core-set approach. In *International Conference on Learning Representations*, 2018.
- [32] Burr Settles. Active learning literature survey. Technical report, University of Wisconsin-Madison Department of Computer Sciences, 2009.
- [33] Zheyang Shen, Jiashuo Liu, Yue He, Xingxuan Zhang, Renzhe Xu, Han Yu, and Peng Cui. Towards out-of-distribution generalization: A survey. *arXiv preprint arXiv:2108.13624*, 2021.
- [34] Rohan Taori, Achal Dave, Vaishaal Shankar, Nicholas Carlini, Benjamin Recht, and Ludwig Schmidt. Measuring robustness to natural distribution shifts in image classification. In *Advances in Neural Information Processing Systems*, volume 33, pages 18583–18599, 2020.
- [35] Damien Teney, Ehsan Abbasnejad, and Anton van den Hengel. Evading the simplicity bias: Training robust ensembles with random weights. In *Proceedings of the IEEE/CVF Conference on Computer Vision and Pattern Recognition*, pages 15410–15419, 2022.
- [36] Eric Tzeng, Judy Hoffman, Kate Saenko, and Trevor Darrell. Adversarial discriminative domain adaptation. In *Proceedings of the IEEE conference on computer vision and pattern recognition*, pages 7167–7176, 2017.

- [37] Olivia Wiles, Sven Gowal, Florian Stimberg, Sylvestre-Alvise Rebuffi, Ira Ktena, Krishnamurthy Dvijotham, and Ali Taylan Cemgil. A fine-grained analysis on distribution shift. In *International Conference on Machine Learning*, pages 23692–23710. PMLR, 2022.
- [38] Daochen Zha, Zaid Pervaiz Bhat, Kwei-Herng Lai, Fan Yang, Zhimeng Jiang, Shaochen Zhong, and Xia Hu. Data-centric artificial intelligence: A survey. *IEEE Transactions on Knowledge and Data Engineering*, 35(12):11442–11458, 2023.

A Mathematical Analysis of Negative Correlation

This appendix provides the mathematical derivation of the negative correlation condition between ID and OOD errors presented in Section 3.2.

Proposition 1 *Let bias parameter b follow a half-normal distribution with scale parameter k , and let error components be defined as $T(b) = b^2$ and $U(b) = (b - \Delta)^2$. The Pearson correlation coefficient between $T(b)$ and $U(b)$ is negative if and only if $k < \alpha\Delta$.*

Proof 1 *The moment generating function of the half-normal distribution with scale parameter k is:*

$$M(t) = \exp\left(\frac{k^2 t^2}{2}\right) \left[1 + \operatorname{erf}\left(\frac{kt}{\sqrt{2}}\right)\right] \quad (13)$$

From this, we derive the raw moments:

$$\mathbb{E}[b^n] = \begin{cases} \alpha k^n (n-1)!!, & \text{if } n \text{ is odd} \\ k^n (n-1)!!, & \text{if } n \text{ is even} \end{cases} \quad (14)$$

For our analysis, we need the first four moments:

$$\mathbb{E}[b] = \alpha k, \quad \mathbb{E}[b^2] = k^2, \quad \mathbb{E}[b^3] = 2\alpha k^3, \quad \mathbb{E}[b^4] = 3k^4 \quad (15)$$

The Pearson correlation coefficient is defined using expectations as:

$$\rho_{X,Y} = \frac{\operatorname{Cov}(X,Y)}{\sigma_X \sigma_Y} = \frac{\mathbb{E}[(X - \mu_X)(Y - \mu_Y)]}{\sqrt{\mathbb{E}[(X - \mu_X)^2] \mathbb{E}[(Y - \mu_Y)^2]}} \quad (16)$$

where $\mu_X = \mathbb{E}[X]$, $\mu_Y = \mathbb{E}[Y]$ are the means, $\sigma_X = \sqrt{\mathbb{E}[(X - \mu_X)^2]}$, $\sigma_Y = \sqrt{\mathbb{E}[(Y - \mu_Y)^2]}$ are the standard deviations, and $\operatorname{Cov}(X,Y) = \mathbb{E}[(X - \mu_X)(Y - \mu_Y)]$ is the covariance.

For our specific case with $T(b) = b^2$ and $U(b) = (b - \Delta)^2$, after simplifying, the covariance between $T(b)$ and $U(b)$ is:

$$\operatorname{Cov}(T,U) = 2k^3(k - \alpha\Delta) \quad (17)$$

The Pearson correlation coefficient is:

$$\rho_{T,U} = \frac{k - \alpha\Delta}{\sqrt{k^2 - 2\alpha\Delta k + \left(2 - \frac{4}{\pi}\right) \Delta^2}} \quad (18)$$

Since the denominator is always positive for $k > 0$, the correlation $\rho_{T,U}$ is negative precisely when $k < \alpha\Delta$.

This negative correlation condition defines the regime where deliberately increasing ID bias improves OOD performance. The correlation $\rho_{T,U}$ is strictly increasing in k throughout $(0, +\infty)$. As k increases from its minimal feasible positive values toward ∞ , $\rho_{T,U}$ increases from approximately -0.936 to 1 , with the strongest negative correlation achieved at the smallest feasible values of $k > 0$.

B Experimental Parameter Details

This appendix provides detailed parameter information for our experimental setup, including both the distribution shift level thresholds and the W_1 distances between distributions.

B.1 Distribution Shift Level Parameters

Permutations in our experiments were categorized into three levels based on their deviation patterns from the global training distribution. Table 3 shows the threshold values used for this categorization.

Table 3: Distribution shift level thresholds for both computational approaches

Approach	Dataset	Threshold	τ Value	Probability
Batchwise	T1S1	τ_{low}	3	0.35
		τ_{high}	6	0.31
	MSD	τ_{low}	2	0.14
		τ_{high}	7	0.16
Cumulative	T1S1	τ_{low}	3	0.68
		τ_{high}	13	0.11
	MSD	τ_{low}	6	0.76
		τ_{high}	14	0.11

Permutations are categorized as Low if outlier count $\leq \tau_{\text{low}}$, Medium if $\tau_{\text{low}} < \text{count} \leq \tau_{\text{high}}$, and High if count $> \tau_{\text{high}}$.

B.2 Dataset Distribution Shift Characteristics

To quantify the magnitude of distribution shifts in our experiments, we measured the W_1 distances in label space between training and test distributions, as shown in Table 4.

Table 4: W_1 distances in label space for ID and OOD settings

Dataset	ID Distance	OOD Distance
T1S1	0.02	0.77
MSD	0.01	0.86

Table 5: Performance comparison across deviation groups on T1S1

Approach	Deviation	Metric	Value	PR (%)
Batchwise	Low	MAE	0.436 ± 0.011	73.3
		RMSE	0.535 ± 0.010	68.9
	Medium	MAE	0.466 ± 0.010	48.9
		RMSE	0.564 ± 0.009	38.9
	High	MAE	0.426 ± 0.008	81.1
		RMSE	0.519 ± 0.007	81.1
Cumulative	Low	MAE	0.403 ± 0.004	87.6
		RMSE	0.496 ± 0.005	87.1
	Medium	MAE	0.397 ± 0.009	88.8
		RMSE	0.490 ± 0.007	90.6
	High	MAE	0.436 ± 0.004	57.3
		RMSE	0.530 ± 0.003	60.0

The significant difference between ID and OOD distances confirms the presence of meaningful distribution shifts in our experimental setup. We maintained OOD distances greater than 0.6 to ensure distribution shifts were substantial enough for evaluation, while keeping ID distances lower to reflect standard cross-validation scenarios. All measurements were computed after separate normalization of training and test sets, which reflects realistic deployment scenarios where test distribution parameters are not available during training.

B.3 Detailed Performance by Deviation Group

Table 5 provides a detailed breakdown of the performance (MAE and RMSE) for each deviation group identified by the ADB framework on the T1S1 dataset. This data supports the analysis presented in Section 5.2, illustrating the performance differences that arise from varying levels of induced distributional diversity during training. Similar patterns can be observed for the MSD dataset in Table 6.

Table 6: Performance comparison across deviation groups on MSD

Approach	Deviation	Metric	Value	PR (%)
Batchwise	Low	MAE	0.860 ± 0.001	60.5
		RMSE	1.153 ± 0.001	53.6
	Medium	MAE	0.856 ± 0.001	79.0
		RMSE	1.148 ± 0.002	71.4
	High	MAE	0.860 ± 0.001	60.5
		RMSE	1.158 ± 0.001	32.1
Cumulative	Low	MAE	0.848 ± 0.001	95.0
		RMSE	1.144 ± 0.007	83.5
	Medium	MAE	0.859 ± 0.001	71.3
		RMSE	1.148 ± 0.001	77.2
	High	MAE	0.863 ± 0.001	62.5
		RMSE	1.152 ± 0.001	63.3

B.4 Statistical Significance Analysis

To validate the statistical significance of our performance improvements, we conducted paired t-tests comparing the ADB approach against traditional cross-validation. Table 7 presents the p-values resulting from these tests across all datasets and computational approaches. Results with $p < 0.05$ indicate statistically significant performance differences, providing strong evidence that the observed improvements are not due to random variation.

Table 7: Statistical significance (p-values from paired t-tests) of ADB compared to CV

Method	Dataset	Metric	p-value	Significant ($p < 0.05$)
Batchwise	T1S1	MAE	$1.4e-5$	Yes
		RMSE	$5.2e-5$	Yes
	MSD	MAE	$5.6e-5$	Yes
		RMSE	$3.7e-4$	Yes
Cumulative	T1S1	MAE	$<1.0e-6$	Yes
		RMSE	$6.0e-6$	Yes
	MSD	MAE	$<1.0e-6$	Yes
		RMSE	$<1.0e-6$	Yes

We assessed statistical significance using 10-fold cross-validation with fixed random seeds, analyzing OOD errors across all folds. This methodology accounts for fold-specific variations while ensuring fair comparison between methods, confirming that our performance improvements are consistent across multiple datasets and evaluation metrics.